Biochemical and Biophysical Research Communications 450 (2014) 1351–1357

Contents lists available at ScienceDirect

Biochemical and Biophysical Research Communications

journal homepage: www.elsevier.com/locate/ybbrc

Impaired expression of caveolin-1 contributes to hepatic ischemia and reperfusion injury

Jung-Woo Kang, Sun-Mee Lee *

School of Pharmacy, Sungkyunkwan University, Suwon 440-746, Republic of Korea

ARTICLE INFO

Article history:
Received 16 June 2014
Available online 2 July 2014

Keywords:
Apoptosis
Caveolae
Caveolin-1
Ischemia and reperfusion
Sphingosine-1-phosphate

ABSTRACT

Caveolae are membrane structures enriched in glycosphingolipids and cholesterol, and caveolin-1 (Cav-1) has been recognized to be pivotal in ischemic tolerance. Sphingosine-1-phosphate (S1P), one of the sphingolipid metabolites, is well known for its anti-apoptotic properties, counteracting ischemia and reperfusion (IR) injury. Here, we investigated the cytoprotective mechanism of Cav-1 against IR injury. Male C57BL/6 mice underwent 70% hepatic ischemia for 60 min, followed by reperfusion. Mice were pretreated with methyl-beta-cyclodextrin (MβCD, 10, 25 and 50 mg/kg, i.p.), a caveolae disruptor, or saline 48 and 24 h before ischemia. Serum and liver tissues were collected at the end of ischemia, at 0, 1, 4 and 24 h of reperfusion. Decreases in the expression of Cav-1 protein and in the number of caveolae of the liver ultrastructure were observed during IR, which were augmented by pretreatment with MβCD. MβCD also augmented the IR-induced increases in serum alanine aminotransferase and tumor necrosis factor-α levels. IR decreased the levels of sphingosine kinase 2 (SK2) and S1P receptor 2 ($S1P_2$) mRNA expressions, while MβCD also augmented these decreases. Moreover, IR resulted in increases of mitochondrial cytochrome *c* release, caspase 3, 8 activities and Bax/Bcl-xL ratio, and MβCD augmented all of these apoptotic parameters. MβCD also increased p38 MAPK and JNK phosphorylation, but did not affect ERK and PI3K/Akt. Our findings demonstrate that downregulation of Cav-1 mediates IR-induced liver damage by inhibiting SK2/$S1P_2$ signaling and enhancing the apoptotic pathway.

1. Introduction

Hepatic ischemia and reperfusion (IR) injury is clinically relevant in liver transplantation, hypovolemic shock, and in some types of toxic injury. Lipid rafts, sphingolipid- and cholesterol-rich domains of the plasma membrane, have been shown to undergo profound alterations in response to acute hypoxic injury due to cholesterol compartmentalization [1]. In particular, the IR-induced rupture of hepatocytes causes the release of intracellular and membrane-bound molecules into the extracellular milieu, contributing to the environmental changes involved in various signaling cascades and hepatocellular damage [2]. Our previous study showed that apoptotic activity is strongly correlated to the extent of IR injury [3].

Caveolae are flask-like lipid rafts that create signaling microdomains, thereby providing spatial and temporal organization of cellular events. Caveolins (Cav-1, -2 and -3), the structural proteins found in caveolae, serve as scaffolds and regulators of signaling proteins [4]. Cav-1 appears to be a hepatocyte fate determinant, inferring resistance to apoptosis [5], and it participates in cell survival and proliferation by modulation of mitogen-activated protein kinases (MAPKs), phosphoinositide 3-kinase (PI3K), and the non-canonical Wnt pathways [6]. Cav-1 has been shown to be involved in the pathogenesis of organ damage in the models of myocardial infarction [7]. Moreover, Lee et al. [8] previously reported that mild IR insult increased the hepatic Cav-1 protein expression, leading to inhibition of endothelial nitric oxide synthase (eNOS) and subsequent impairment of nitric oxide production. However, the pattern changes of Cav-1 and its exact role in IR-induced hepatocellular damage are still unclear.

Signaling lipids such as ceramide and glycosphingolipid are enriched in caveolae, and sphingosine-1-phosphate (S1P) functions as both an extracellular ligand for G protein-coupled S1P receptors ($S1P_1$–$S1P_5$) and an intracellular second messenger in promoting cell growth and survival, and the inhibition of apoptosis [9]. Altered sphingolipid metabolism occurs in ischemic injury, and its functional significance has been reported; for example, downregulation of sphingosine kinases (SKs) and $S1P_1$ were founded in the infarct cortex after cerebral ischemia, while activation of the

* Corresponding author. Address: School of Pharmacy, Sungkyunkwan University, Seobu-ro 2066, Jangan-gu, Suwon, Gyeonggi-do 440-746, Republic of Korea. Fax: +82 31 292 8800.
E-mail address: sunmee@skku.edu (S.-M. Lee).

http://dx.doi.org/10.1016/j.bbrc.2014.06.131
0006-291X/

sphingosine metabolic pathway was suggested to be neuroprotective [10]. In addition, the sphingomyelinase inhibitor, desipramine, was found to prevent myocardial ischemic injury by attenuating ceramide accumulation and the interaction between eNOS and Cav-1 [11].

In this study, we aimed to investigate the time-dependent changes in expression of Cav-1, the role of Cav-1 in hepatic IR injury and its molecular mechanisms linked to S1P signaling and apoptotic cell death.

2. Materials and methods

2.1. Chemicals and antibodies

Methyl-β-cyclodextrin (MβCD) was purchased from Sigma–Aldrich (St. Louis, MO, USA). Cav-1 antibody was purchased from Santa Cruz Biotechnology (Santa Cruz, CA, USA). The following antibodies were purchased from Cell Signaling Technology (Danvers, MA, USA): cytochrome *c*, Bax, Bcl-xL, total- and phosphorylated (p−) p38 MAPK, c-Jun N-terminal kinases (JNK), ERK, PI3K and Akt. The *β*-actin antibody was purchased from Sigma–Aldrich.

2.2. Hepatic IR procedure and MβCD treatment

All animals received care in compliance with both the Principles of Laboratory Animal Care formulated by the National Institutes of Health (NIH publication No.86-23, revised 1985) and the guidelines of the Sungkyunkwan University Animal Care Committee. Male C57BL/6 mice weighing 22–24 g were obtained from Orient Bio Inc. (Seongnam, Korea), and were acclimatized to laboratory conditions at least one week prior to initiating experiments. Mice were anesthetized with ketamine (100 mg/kg, i.m.) and xylazine (10 mg/kg, i.m.). The left branches of the portal vein and hepatic artery were clamped to induce complete ischemia of the median and left lobes of the liver. After 60 min of ischemia, the clamp was removed to allow reperfusion for 0 (immediately after declamping), 1, 4 and 24 h. Sham-operated mice were prepared in a similar manner; however, a clip was not placed on the vasculature. After IR injury, mice were sacrificed and blood from the inferior vena cava and liver tissue was collected. MβCD was dissolved in saline and administered 48 h and 24 h prior to ischemia (at concentrations of 10, 25 and 50 mg/kg of body weight, i.p.). The dosage and timing of MβCD administration were selected based on a previous report [12], as well as on preliminary investigations in our laboratory.

2.3. Serum alanine aminotransferase (ALT), tumor necrosis factor (TNF)-α and cytosolic caspase-3 and -8 activities

Serum ALT activity was measured with a ChemiLab ALT assay kit (IVDLab Co., Uiwang, Korea). Serum TNF-α levels were quantified by an enzyme-linked immunosorbent assay (ELISA) using a commercial TNF-α ELISA assay kit (BD Biosciences Co., San Jose, CA, USA). Caspase activities were measured using an *in vitro* colorimetric peptide substrate, namely, Ac-Asp-Glu-Val-Asp p-nitroanilide for a caspase-3 substrate peptide and Ac-Ile-Glu-Thr-Asp p-nitroaniline for a caspase-8 substrate peptide (DEVD-AFC; Bio-Mol, Plymouth Meeting, PA, USA). A sample of liver tissue was then homogenized in buffer containing 25 mM Tris, 5 mM $MgCl_2$, and 1 mM EGTA. The homogenate was centrifuged for 15 min at 40,000*g*, and the resulting supernatant was collected for determination of caspase activities according to the manufacturer's instructions.

2.4. Liver ATP and its catabolites analysis

The median lobe of liver samples was frozen in liquid nitrogen and freeze-dried. The tissue was then minced to a powder and extracted with 1.5 M perchloric acid. Following centrifugation, neutralization and final centrifugation, extracts were kept in an ice bath until injected into a high-performance liquid chromatography (Gilson model) system for analysis. The hepatic concentrations of ATP, ADP and AMP were measured based on our previous study [13]. Energy charge (EC) was calculated as EC = (ATP + 1/2 ADP)/(ATP + ADP + AMP).

2.5. Hematoxylin and eosin (H&E) staining and terminal dUTP nick-end labeling (TUNEL) assay

Liver specimens were fixed in 10% buffered formalin, embedded in paraffin, and stained with H&E. The stained sections were blindly examined using a light microscope (Olympus CKX41, Olympus Optical Co., Tokyo, Japan). The criteria reported by Suzuki et al. were utilized [14]. In this classification, 3 liver injury indices were graded: sinusoidal congestion (score: 0–4), hepatocyte necrosis (score: 0–4), and ballooning degeneration (score: 0–4), total score of 0–12. Apoptotic cells were detected by TUNEL staining with a commercially available kit (ApopTag® *In Situ* Apoptosis Detection Kits, Millipore, Billerica, MA, USA). Apoptosis of hepatocytes in liver sections was quantitated by counting the number of TUNEL-positive cells in random microscopic high-power fields (×100).

2.6. Western blot analysis

Liver tissue protein lysates were prepared using PRO-PREP™ protein extraction solution (iNtRON Biotechnology Inc., Seongnam, Korea) for total fractions and NE-PER (Pierce Biotechnology, Rockford, IL) for cytosolic fractions according to the manufacturer's instructions [15]. Western blotting was performed using primary antibodies and horseradish peroxidase-conjugated secondary antibodies suitable for each primary antibody. Detection was carried out using the WEST-one Western Blot Detection System (iNtRON Biotechnology Inc.), according to the manufacturer's instructions. Intensities of the immunoreactive bands were determined using TotalLab TL120 software (IVDLab Nonlinear Dynamics Co. Ltd., Newcastle, UK). *β*-Actin was used as a loading control, and protein levels were normalized to the corresponding *β*-actin band intensity.

2.7. Transmission electron microscopy (TEM)

TEM was performed on liver tissue samples, as previously described [16]. Caveolae structures were observed in blinded samples using a transmission electron microscope (JEM-1010, JEOL, Tokyo, Japan).

2.8. Quantitative real-time polymerase chain reaction (PCR) analysis

Total RNA was extracted from liver tissue using RNA isoPlus (Takara Bio Inc., Shiga, Japan), followed by cDNA synthesis through reverse transcription (EcoDry™ cDNA Synthesis Premix, Takara Bio Inc.). The cDNA was amplified by real-time PCR with a thermocycler (Lightcycler® Nano, Roche Applied Science, Indianapolis, IN, USA) and a SYBR Green detection system (Roche Applied Science, Mannheim, Germany). The gene-specific primers were as follows (5′ → 3′): Cav-1, sense: AGACTCCGAGGGACATCTC, anti-sense: GCGTCATACACTTGCTTCTC; SK1, sense: GGCTCTGCAGCTCTTCCAGAG, anti-sense: CTCCTCTGCACACACCAGCTC; SK2, sense: CGGAT-

GCCCATTGGTGTCCTC, anti-sense: TGAGCAACAGGTCAACACCGAC; $S1P_1$, sense: TTCTCATCTGCTGCTTCATCATCC, anti-sense: GGTCCGAGAGGGCTAGGTTG; $S1P_2$, sense: TTACTGGCTATCGTGGCTCTG, anti-sense: ATGGTGACCGTCTTGAGCAG; and β-actin, sense: TGGAATCCTGTGGCATCCAT, anti-sense: TAAAACGCAGCTCAGTAACA. The mRNA expression levels were normalized to the expression level of β-actin mRNA, and relative to the average of all delta Ct-values in each sample using the cycle threshold (Ct) method. All experiments were conducted in duplicate to ensure amplification integrity.

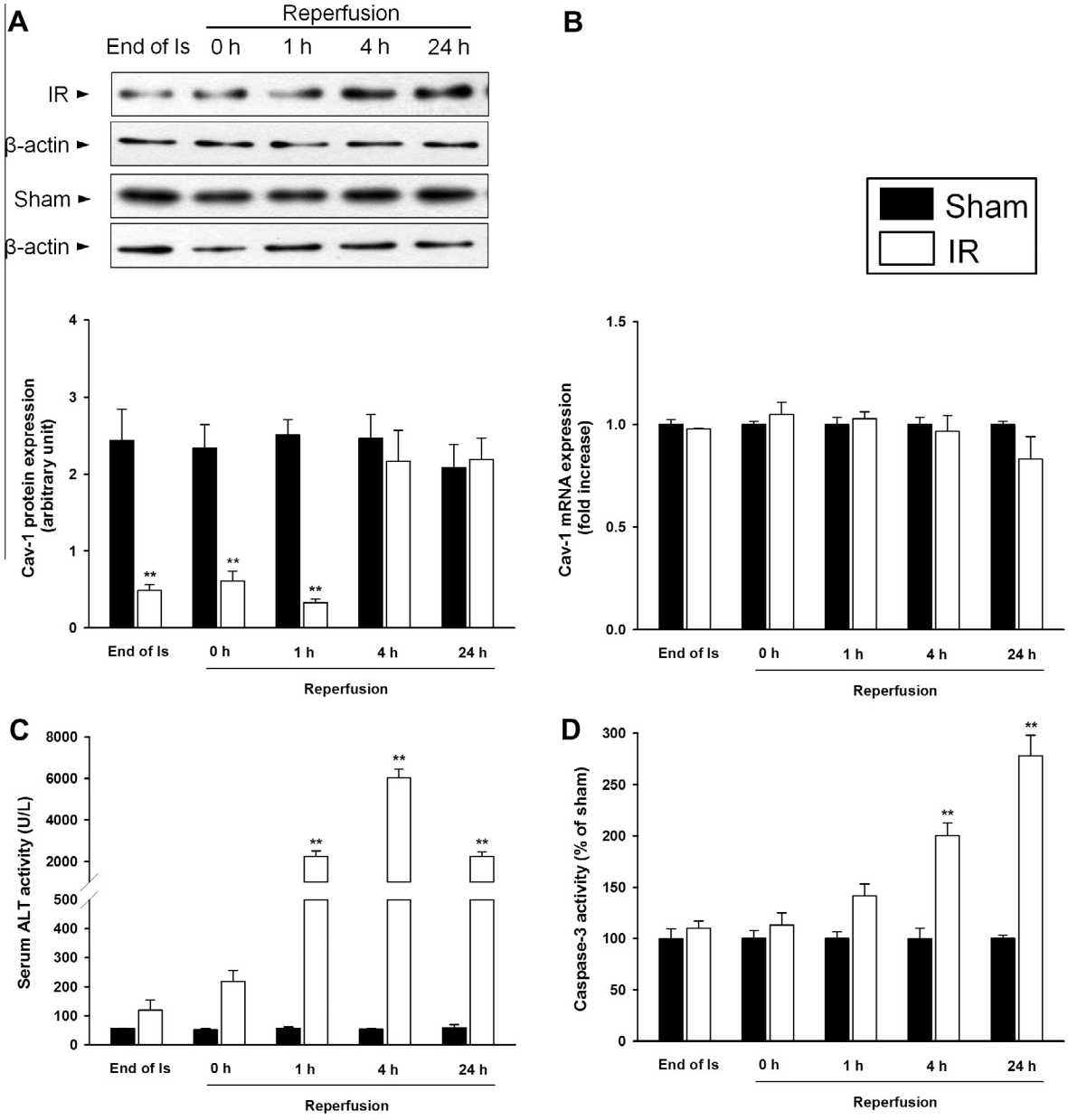

Fig. 1. Time course changes of Cav-1 expression during IR. Western blot analysis and quantitative real time-PCR were performed to measure hepatic Cav-1 protein and mRNA expression, respectively (A and B). Hepatocellular damage was demonstrated by serum ALT activity (C) and cytosolic caspase-3 activity (D). Results are presented as mean ± S.E.M. of 8–10 animals per group. **Denotes significant differences ($P < 0.01$) compared with the sham group.

Table 1
Changes in ATP contents and energy charge during liver IR.

	Group	End of ischemia	0 h Reperfusion	1 h Reperfusion	4 h Reperfusion	24 h Reperfusion
ATP contents (μmol/g liver)	Sham	6.83 ± 0.53	6.70 ± 0.58	6.54 ± 0.67	7.00 ± 0.99	6.90 ± 0.72
	IR	1.50 ± 0.21**	2.19 ± 0.20**	2.21 ± 0.15**	3.14 ± 0.10**	4.21 ± 0.23*
EC	Sham	0.68 ± 0.09	0.66 ± 0.07	0.64 ± 0.07	0.62 ± 0.10	0.67 ± 0.09
	IR	0.29 ± 0.07**	0.39 ± 0.05*	0.43 ± 0.05*	0.56 ± 0.05	0.61 ± 0.04

The values are represented as means ± S.E.M. for 8–10 mice per group. *,**Denote significant differences ($P < 0.05$, $P < 0.01$) compared with the sham group. EC was calculated as EC = (ATP + 1/2 ADP)/(ATP + ADP + AMP). EC: energy charge.

2.9. Statistical analysis

All results are presented as the mean ± S.E.M. The overall significance of the data was tested by two-way analysis of variance using the SPSS v.12.0 statistical software package (SPSS, Chicago, IL, USA). Differences between groups were considered statistically significant at $P < 0.05$ with appropriate Bonferroni corrections made for multiple comparisons.

3. Results

3.1. Time course changes of Cav-1 expressions during IR

Pattern changes of Cav-1 protein and mRNA expressions were initially observed during IR. Ischemia itself reduced the level of Cav-1 protein expression, which persisted for 1 h after reperfusion. However, the decreased Cav-1 protein expression recovered to

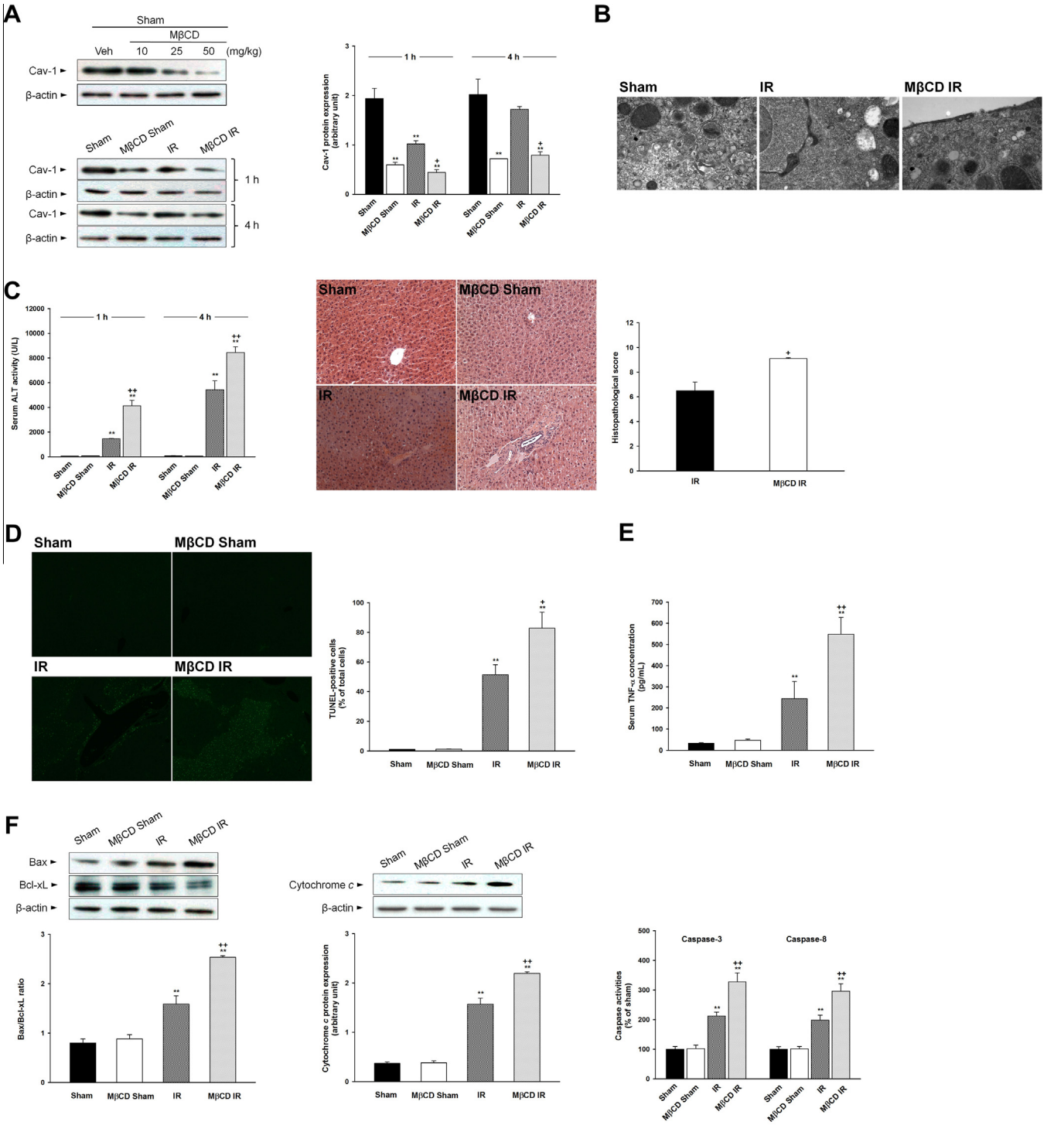

Fig. 2. Effects of MβCD on hepatocellular damage in IR. Western blot analysis was performed to measure hepatic Cav-1 protein expression (A). After 1 h of reperfusion, caveolae structure was observed by TEM (B). Serum ALT activities and pathological scores of H&E staining pictures were demonstrated (C). TUNEL-positive hepatocytes were counted (D) and serum TNF-α activity was measured by a commercial ELISA kit after 4 h of reperfusion (E). After 4 h of reperfusion, cytosolic Bax/Bcl-xL ratio, cytochrome *c* and caspase 3 and 8 activities (F) were measured as apoptotic markers. Results are presented as mean ± S.E.M. of 8–10 animals per group. **Denote significant differences ($P < 0.01$), compared with the sham group. +,++Denote significant differences ($P < 0.05$, $P < 0.01$), compared with the IR group.

basal levels after 4 h, and was maintained until 24 h of reperfusion. No significant changes in Cav-1 mRNA expression were observed among any of the experimental groups (Fig. 1A–B).

Representative markers for cell damage as well as energy metabolism during IR are shown in Fig. 1C, D and Table 1. At the end of the ischemic period and immediately after reperfusion, serum ALT activities were not different from those of sham-operated animals. However, the serum ALT activity significantly increased after 1 h of reperfusion, peaking at 4 h. ALT activity then declined until 24 h of reperfusion. The caspase-3 activity of the cytosolic fractions obtained from both the sham-operated and ischemic animals was quite low. However, the caspase-3 activity in ischemic animals was higher after 1 h of reperfusion, peaking after 4 h. This increased caspase-3 activity was sustained until 24 h of reperfusion. Moreover, the value of cellular ATP in the liver of sham-operated animals was 6.83 ± 0.53 μmol/g liver, while it decreased rapidly after 60 min of ischemia (1.50 ± 0.21 μmol/g liver). After 1 and 4 h of reperfusion, hepatic ATP levels had increased and were found to be approximately 33.8% and 44.9% of those seen in the sham-operated animals, respectively. The hepatic energy charge was significantly reduced immediately after the 60 min of ischemia. In the IR group, however, the energy charge was restored to the level of the sham-operated animals after 4 h of reperfusion.

3.2. Effects of MβCD on hepatocellular damage in IR

While the 10 mg/kg of MβCD showed a slight tendency to decrease the level of Cav-1 protein expression, 25 and 50 mg/kg of MβCD significantly decreased the Cav-1 protein expression in sham-operated animals. Therefore, MβCD at 25 mg/kg was chosen for the following studies. The MβCD was found to augment the decrease in Cav-1 expression observed after 1 h of reperfusion. After 4 h of reperfusion, while no difference in Cav-1 protein expression was seen in IR animals compared to sham-operated animals, the MβCD-treated animals demonstrated decreased Cav-1 expression compared to the IR animals (Fig. 2A). By EM analysis, the decrease in the number of caveolae membrane structure after 1 h of reperfusion was also augmented by MβCD (Fig. 2B). In addition, the increased levels of serum ALT after both 1 and 4 h of reperfusion were also augmented by MβCD. H&E stained liver sections were evaluated for the degree of hepatocellular damage using Suzuki's criteria after 1 h of reperfusion. The ischemic lobes in the IR animals showed severe necrosis, sinusoidal congestion and hepatocyte vacuolization, all of which were aggravated by MβCD (Fig. 2C). While no TUNEL-positive cells were detected in sham-operated animals, the level of apoptosis induced by IR was 51.4 ± 6.8%, which was increased to 82.9 ± 10.7% after treatment with MβCD (Fig. 2D). The level of serum TNF-α concentration in the IR group was significantly higher than that in the sham group. This increase was also augmented by MβCD. MβCD was also found to augment the increased cytosolic Bax/Bcl-xL ratio and cytochrome *c* protein expressions, as well as the increase in caspase-3 and -8 activities in the cytosolic fraction after 4 h of reperfusion (Fig. 2E and F).

3.3. Effects of MβCD on MAPK and PI3K/Akt pathways in IR

The levels of p38 MAPK, JNK and ERK phosphorylation significantly increased after 1 h of reperfusion. While p38 MAPK and

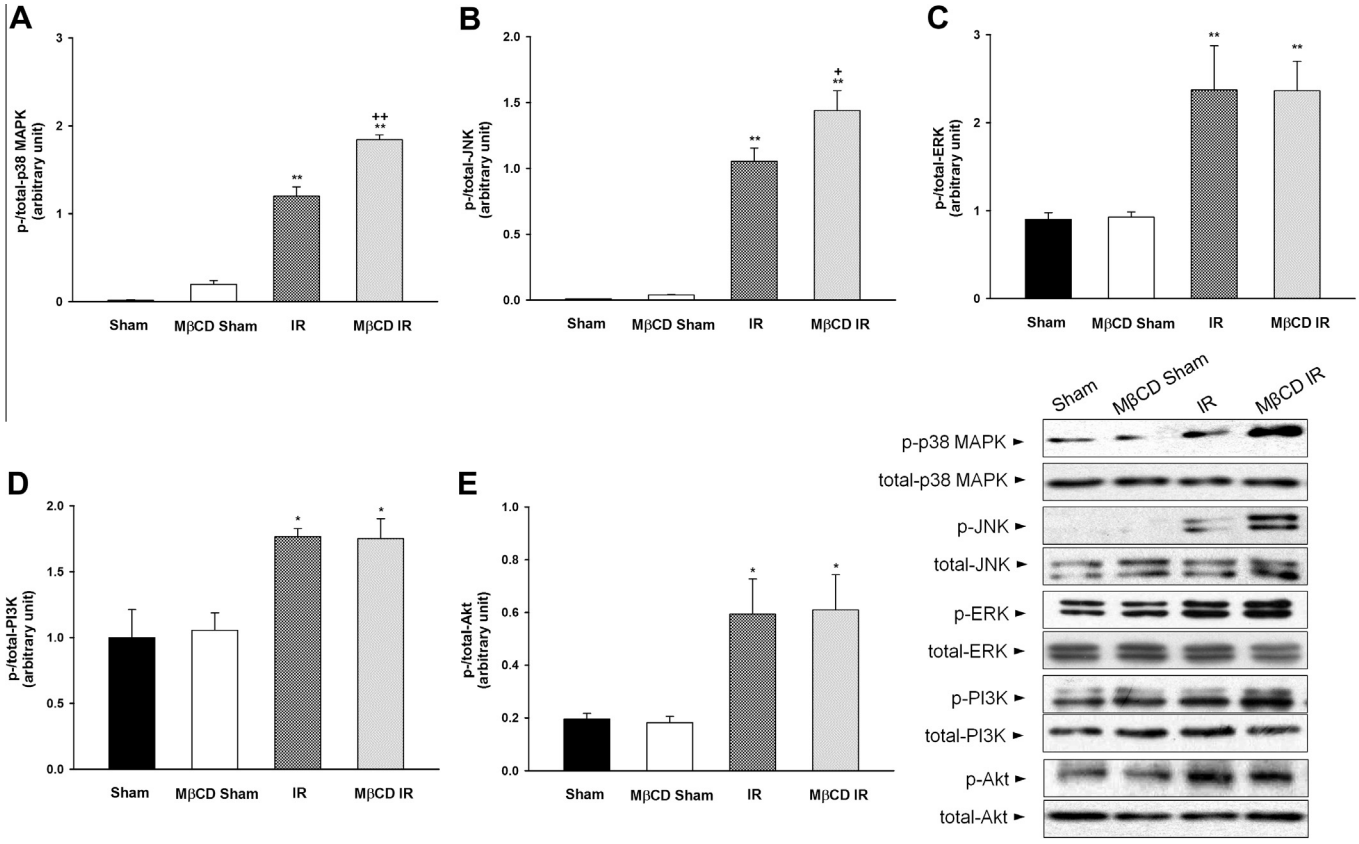

Fig. 3. Effects of MβCD on MAPK and PI3K/Akt pathways in IR. Western blot analysis was performed to measure the phosphorylation of p38 MAPK (A), JNK (B), ERK (C), PI3K (D) and Akt (E) after 1 h of reperfusion. Results are presented as mean ± S.E.M. of 8–10 animals per group. *,**Denote significant differences ($P < 0.05$, $P < 0.01$), compared with the sham group. +,++Denote significant differences ($P < 0.05$, $P < 0.01$), compared with the IR group.

JNK phosphorylation were augmented by MβCD, ERK phosphorylation was unaffected. In addition, while the levels of PI3K and Akt phosphorylation significantly increased after 1 h of reperfusion, these increases were not affected by MβCD (Fig. 3A–E).

3.4. Effects of MβCD on SKs and S1P receptors

While the level of $S1P_1$ mRNA expression was not affected by IR, the levels of SK1, SK2 and $S1P_2$ mRNA expressions significantly decreased after 1 h of reperfusion. The decreases in SK2 and $S1P_2$ mRNA expressions were augmented by MβCD, while the level of SK1 mRNA expression unaffected (Fig. 4A and B).

4. Discussion

Caveolin proteins have been implicated in the pathogenesis of various organ injuries and in conditions such as ischemia, in which a mismatch occurs between energy production and utilization. Such conditions are associated with altered expression of caveolae or redistribution of caveolin; for instance, hypoxic injury imposed on renal proximal tubules causes Cav-1 release, accompanied with caveolae disruption, and Cav-1 appearing within the extracellular space was largely in the denatured form [1]. In the present study,

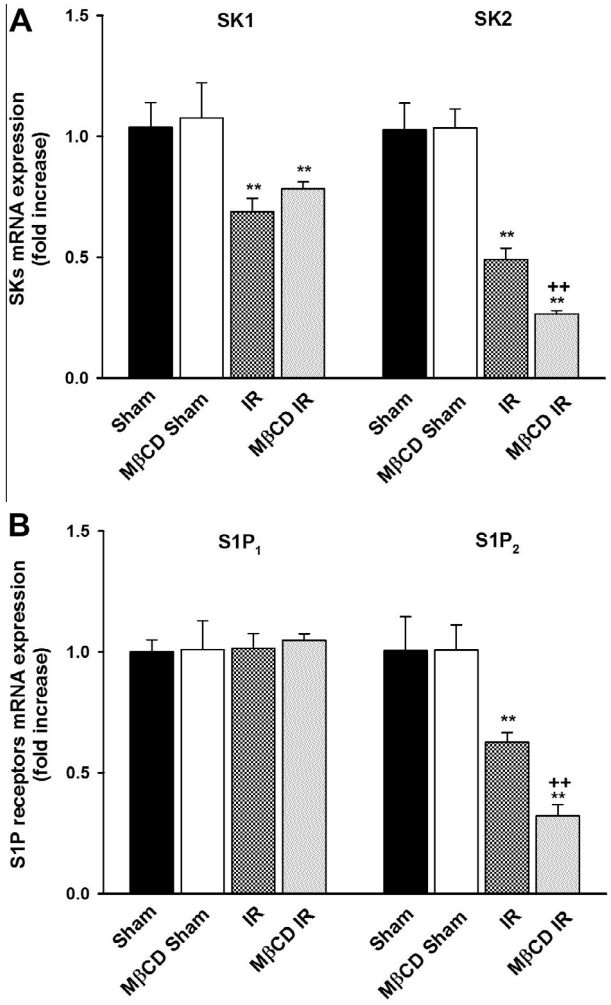

Fig. 4. Effects of MβCD on SKs and S1P receptors. Quantitative real time-PCR was performed to measure the SK1 and SK2 (A) and $S1P_1$ and $S1P_2$ (B) mRNA expressions after 1 h of reperfusion. Results are presented as mean ± S.E.M. of 8–10 animals per group. **Denotes significant differences ($P < 0.01$), compared with the sham group. ++Denotes significant differences ($P < 0.01$), compared with the IR group.

the end of the ischemic period and early phase of reperfusion was characterized by a decrease in hepatic Cav-1 protein expression, which was recovered to basal levels after 4 h of reperfusion. However, Cav-1 mRNA expression remained unchanged throughout the periods. This result indicates that IR downregulates Cav-1 expression at the translational level. In the present study, the status of energy metabolism was one of the most important functional disorders in terms of predicting the viability of the ischemic organs; hepatic ATP content significantly decreased at the end of the ischemic period, and gradually increased during the reperfusion phase. Furthermore, EC, which represents the energy balance between energy production and consumption, was reduced immediately after ischemia, but recovered after reperfusion. Our data showed that a temporal association exists between Cav-1 expression and energy metabolism.

IR injury activates cell death signaling programs including necrosis, apoptosis and autophagy-associated cell death. Among these, apoptosis is of particular interest because it often amplifies inflammatory response [17], and the extent of apoptotic cell death in IR injury correlates with hepatic function [18]. When reperfusion leads to mitochondrial permeability transition onset and ATP depletion, necrosis occurs as a result of the failure of ATP regeneration. In contrast, if glycolytic substrate is available, profound ATP depletion is prevented, instead, ATP-dependent apoptotic signaling occurs [3] which correlates with our present results of caspase-3 activities (Fig. 1D). Recently, Cav-1 has gained attention as a crucial cell fate regulator in hepatocytes, stimulated by transforming growth factor-β, and gene silencing of Cav-1 reduced the expression of anti-apoptotic molecules [5]. Cav-1 also functions as a shear sensor in flow-adapted endothelial cells, resulting in cell proliferation, a compensatory mechanism to restore perfusion, after abrupt reduction in flow [19]. MβCD, a pharmacologic agent, alters the cholesterol content of the plasma membrane, thereby destroying the structure of caveolae [20], inducing high expression of JNK and Bax with low expression of anti-apoptotic molecules such as Bcl-2 and Bcl-xL, even after ischemic preconditioning in the heart [21]. To investigate the role of Cav-1 in the pathogenesis of hepatic IR, loss-of-function study was performed after 1 and 4 h of reperfusion, at which time hepatocellular damage peaked. Treatment with MβCD further decreased the number of caveolae structures in the hepatocytes and Cav-1 protein expression during IR. In addition, MβCD augmented IR-induced apoptotic cell death. These results suggest that impaired Cav-1 contributes to IR-induced apoptotic cell death.

The molecular machinery of apoptosis is highly regulated by intracellular calcium, free radicals, and death receptor ligands such as Fas ligands. The simultaneous activation of prosurvival kinases, including, PI3K/Akt, protein kinase C and ERK, can be induced by cell survival components such as growth factors [22]. Caveolar domains have previously been proposed to interact with pro- and anti-apoptotic signaling molecules; Cav-1-mediated increase in Akt activities were shown to be responsible for the cell survival of prostate cancer cells [23]. Alternatively, silencing of the Cav-1 gene promoted p38 MAPK and JNK activation via toll-like receptor 4 signaling in the response of human mammary epithelial cells to lipopolysaccharide [24]. In the present study, while increases in the phosphorylation of p38 MAPK and JNK were augmented by MβCD, ERK and PI3K/Akt phosphorylation were not affected. Our results suggest that impairment of Cav-1 activates p38 MAPK and JNK during IR.

Sphingolipids, including sphingosine, are essential structural and functional components of the plasma membrane, and its metabolites have various biological roles including in cell death, oncogenesis and inflammation [25]. SK is a conserved lipid kinase with two mammalian isoforms (SK1 and SK2), which catalyze the ATP-dependent phosphorylation of sphingosine to S1P [26].

Previously, protective roles of $S1P_2$ and $S1P_3$ were reported in myocardial IR using double $S1P_2/S1P_3$ knockout mice [27], and SK2 knockout also sensitized the mice to IR-induced cardiac dysfunction [28]. Moreover, S1P receptor agonists such as FTY720 and SEW2871 reduced IR-induced renal injury via inhibition of proximal tubule cell death [29]. Song et al. reported that isoflurane increases caveolae formation in human renal proximal tubule cells, and the caveolae fractions contain vital components of isoflurane-mediated renal protection such as the SK1, S1P and TGF-β1 receptors [30]. In the present study, liver IR decreased expression of SK1, SK2 and $S1P_2$ mRNA, while it did not affect $S1P_1$. Moreover, MβCD augmented the decreases in SK2 and $S1P_2$ mRNA expression. These results indicate that impaired Cav-1 suppresses $SK2/S1P_2$ signaling during IR.

In conclusion, Cav-1 expression is impaired during liver IR, which mediates apoptotic cell death and inhibits $SK2/S1P_2$ signaling. Our findings suggest that Cav-1 might be a potential regulator of hepatocellular damage during liver IR.

Acknowledgments

Jung-Woo Kang received 'Global Ph.D. Fellowship Program' support from the National Research Foundation of Korea (NRF), funded by the Ministry of Education, Science and Technology (MEST) (2011-0006724). This research was supported by the Basic Science Research Program through the National Research Foundation of Korea (NRF) funded by the Ministry of Science, ICT & Future Planning (NRF-2013R1A1A3008145).

References

[1] R.A. Zager, A. Johnson, S. Hanson, V. dela Rosa, Altered cholesterol localization and caveolin expression during the evolution of acute renal failure, Kidney Int. 61 (2002) 1674–1683.
[2] D. Monbaliu, B. de Vries, T. Crabbe, E. van Heurn, C. Verwaest, T. Roskams, J. Fevery, J. Pirenne, W.A. Buurman, Liver fatty acid-binding protein: an early and sensitive plasma marker of hepatocellular damage and a reliable predictor of graft viability after liver transplantation from non-heart-beating donors, Transplant Proc. 37 (2005) 413–416.
[3] H.A. Eum, Y.N. Cha, S.M. Lee, Necrosis and apoptosis: sequence of liver damage following reperfusion after 60 min ischemia in rats, Biochem. Biophys. Res. Commun. 358 (2007) 500–505.
[4] H. Kathuria, Y.X. Cao, M.I. Ramirez, M.C. Williams, Transcription of the caveolin-1 gene is differentially regulated in lung type I epithelial and endothelial cell lines. A role for ETS proteins in epithelial cell expression, J. Biol. Chem. 279 (2004) 30028–30036.
[5] C. Meyer, Y. Liu, A. Kaul, I. Peipe, S. Dooley, Caveolin-1 abrogates TGF-beta mediated hepatocyte apoptosis, Cell Death. Dis. 4 (2013) e466.
[6] H.H. Patel, F. Murray, P.A. Insel, Caveolae as organizers of pharmacologically relevant signal transduction molecules, Annu. Rev. Pharmacol. Toxicol. 48 (2008) 359–391.
[7] H.H. Patel, Y.M. Tsutsumi, B.P. Head, I.R. Niesman, M. Jennings, Y. Horikawa, D. Huang, A.L. Moreno, P.M. Patel, P.A. Insel, D.M. Roth, Mechanisms of cardiac protection from ischemia/reperfusion injury: a role for caveolae and caveolin-1, FASEB J. 21 (2007) 1565–1574.
[8] S.H. Lee, C. Culberson, K. Korneszczuk, M.G. Clemens, Differential mechanisms of hepatic vascular dysregulation with mild vs. moderate ischemia–reperfusion, Am. J. Physiol. 294 (2008) G1219–G1226.
[9] T. Hla, M.J. Lee, N. Ancellin, C.H. Liu, S. Thangada, B.D. Thompson, M. Kluk, Sphingosine-1-phosphate: extracellular mediator or intracellular second messenger?, Biochem Pharmacol. 58 (1999) 201–207.
[10] Y. Hasegawa, H. Suzuki, O. Altay, W. Rolland, J.H. Zhang, Role of the sphingosine metabolism pathway on neurons against experimental cerebral ischemia in rats, Transl. Stroke Res. 4 (2013) 524–532.
[11] M. Salinas, R. Lopez-Valdaliso, D. Martin, A. Alvarez, A. Cuadrado, Inhibition of PKB/Akt1 by C2-ceramide involves activation of ceramide-activated protein phosphatase in PC12 cells, Mol. Cell. Neurosci. 15 (2000) 156–169.
[12] D. Zhu, W.C. Xiong, L. Mei, Lipid rafts serve as a signaling platform for nicotinic acetylcholine receptor clustering, J. Neurosci. 26 (2006) 4841–4851.
[13] B.R. Jeon, S.M. Lee, S-adenosylmethionine protects post-ischemic mitochondrial injury in rat liver, J. Hepatol. 34 (2001) 395–401.
[14] S. Suzuki, L.H. Toledo-Pereyra, F.J. Rodriguez, D. Cejalvo, Neutrophil infiltration as an important factor in liver ischemia and reperfusion injury. Modulating effects of FK506 and cyclosporine, Transplantation 55 (1993) 1265–1272.
[15] J. Park, J.W. Kang, S.M. Lee, Activation of the cholinergic anti-inflammatory pathway by nicotine attenuates hepatic ischemia/reperfusion injury via heme oxygenase-1 induction, Eur. J. Pharmacol. 707 (2013) 61–70.
[16] J.W. Kang, H.I. Cho, S.M. Lee, Melatonin inhibits mTOR-dependent autophagy during liver ischemia/reperfusion, Cell. Physiol. Biochem. 33 (2014) 23–36.
[17] H. Jaeschke, Inflammation in response to hepatocellular apoptosis, Hepatology 35 (2002) 964–966.
[18] G. Borghi-Scoazec, J.Y. Scoazec, F. Durand, J. Bernuau, J. Belghiti, G. Feldmann, D. Henin, C. Degott, Apoptosis after ischemia–reperfusion in human liver allografts, Liver Transpl. Surg. 3 (1997) 407–415.
[19] T. Milovanova, S. Chatterjee, B.J. Hawkins, N. Hong, E.M. Sorokina, K. Debolt, J.S. Moore, M. Madesh, A.B. Fisher, Caveolae are an essential component of the pathway for endothelial cell signaling associated with abrupt reduction of shear stress, Biochim. Biophys. Acta 1783 (2008) 1866–1875.
[20] E.J. Smart, R.G. Anderson, Alterations in membrane cholesterol that affect structure and function of caveolae, Methods Enzymol. 353 (2002) 131–139.
[21] M. Das, M. Gherghiceanu, I. Lekli, S. Mukherjee, L.M. Popescu, D.K. Das, Essential role of lipid raft in ischemic preconditioning, Cell. Physiol. Biochem. 21 (2008) 325–334.
[22] H. Malhi, G.J. Gores, J.J. Lemasters, Apoptosis and necrosis in the liver: a tale of two deaths?, Hepatology 43 (2006) S31–S44
[23] L. Li, C.H. Ren, S.A. Tahir, C. Ren, T.C. Thompson, Caveolin-1 maintains activated Akt in prostate cancer cells through scaffolding domain binding site interactions with and inhibition of serine/threonine protein phosphatases PP1 and PP2A, Mol. Cell. Biol. 23 (2003) 9389–9404.
[24] X.X. Wang, Z. Wu, H.F. Huang, C. Han, W. Zou, J. Liu, Caveolin-1, through its ability to negatively regulate TLR4, is a crucial determinant of MAPK activation in LPS-challenged mammary epithelial cells, Asian Pac. J. Cancer Prev. 14 (2013) 2295–2299.
[25] S.K. Jo, A. Bajwa, A.S. Awad, K.R. Lynch, M.D. Okusa, Sphingosine-1-phosphate receptors: biology and therapeutic potential in kidney disease, Kidney Int. 73 (2008) 1220–1230.
[26] H. Le Stunff, S. Milstien, S. Spiegel, Generation and metabolism of bioactive sphingosine-1-phosphate, J. Cell. Biochem. 92 (2004) 882–899.
[27] C.K. Means, C.Y. Xiao, Z. Li, T. Zhang, J.H. Omens, I. Ishii, J. Chun, J.H. Brown, Sphingosine 1-phosphate S1P2 and S1P3 receptor-mediated Akt activation protects against *in vivo* myocardial ischemia–reperfusion injury, Am. J. Physiol. 292 (2007) H2944–H2951.
[28] D.A. Vessey, L. Li, Z.Q. Jin, M. Kelley, N. Honbo, J. Zhang, J.S. Karliner, A sphingosine kinase form 2 knockout sensitizes mouse myocardium to ischemia/reoxygenation injury and diminishes responsiveness to ischemic preconditioning, Oxid. Med. Cell. Longev. 2011 (2011) 961059.
[29] A. Bajwa, S.K. Jo, H. Ye, L. Huang, K.R. Dondeti, D.L. Rosin, V.H. Haase, T.L. Macdonald, K.R. Lynch, M.D. Okusa, Activation of sphingosine-1-phosphate 1 receptor in the proximal tubule protects against ischemia–reperfusion injury, J. Am. Soc. Nephrol. 21 (2010) 955–965.
[30] J.H. Song, M. Kim, S.W. Park, S.W. Chen, S.M. Pitson, H.T. Lee, Isoflurane via TGF-beta1 release increases caveolae formation and organizes sphingosine kinase signaling in renal proximal tubules, Am. J. Physiol. 298 (2010) F1041–F1050.